

TPPO: A Novel Trajectory Predictor with Pseudo Oracle

Biao Yang, *Member, IEEE*, Guocheng Yan, Pin Wang, *Member, IEEE*, Ching-Yao Chan, *Member, IEEE*, Xiaofeng Liu, *Member*, Yang Chen, *Member, IEEE, IEEE*

Abstract—Forecasting pedestrian trajectories in dynamic scenes remains a critical problem with various applications, such as autonomous driving and socially aware robots. Such forecasting is challenging due to human—human and human—object interactions and future uncertainties caused by human randomness. Generative model-based methods handle future uncertainties by sampling a latent variable. However, few previous studies carefully explored the generation of the latent variable. In this work, we propose the *Trajectory Predictor with Pseudo Oracle* (TPPO), which is a generative model-based trajectory predictor. The first pseudo oracle is pedestrians’ moving directions, and the second one is the latent variable estimated from observed trajectories. A social attention module is used to aggregate neighbors’ interactions on the basis of the correlation between pedestrians’ moving directions and their future trajectories. This correlation is inspired by the fact that a pedestrian’s future trajectory is often influenced by pedestrians in front. A latent variable predictor is proposed to estimate latent variable distributions from observed and ground-truth trajectories. Moreover, the gap between these two distributions is minimized during training. Therefore, the latent variable predictor can estimate the latent variable from observed trajectories to approximate that estimated from ground-truth trajectories. We compare the performance of TPPO with related methods on several public datasets. Results demonstrate that TPPO outperforms state-of-the-art methods with low average and final displacement errors. Besides, the ablation study shows that the prediction performance will not dramatically decrease as sampling times decline during tests.

Index Terms—trajectory prediction, latent variable predictor, social attention, generative adversarial network, future uncertainty.

I. INTRODUCTION

Forecasting pedestrian trajectories in dynamic scenes remains a critical problem with various applications, such as autonomous driving [1], social behavior-aware robots [2], and intelligent tracking system [3]. Fig. 1 shows a typical scenario of trajectory prediction. Pedestrians’ future trajectories labeled with different colored arrows are predicted on the basis of past trajectories labeled with different colored lines. A human observer can most likely forecast that the woman (blue) with a shoulder bag will turn right to avoid the still car. However, a robot without prior knowledge or solid training may not do

the same thing because it does not quite understand human—human and human—object interactions. Several inherent human properties, including interpersonal, socially acceptable, and multi-modal properties also pose critical challenges for robots to perform accurate trajectory prediction.

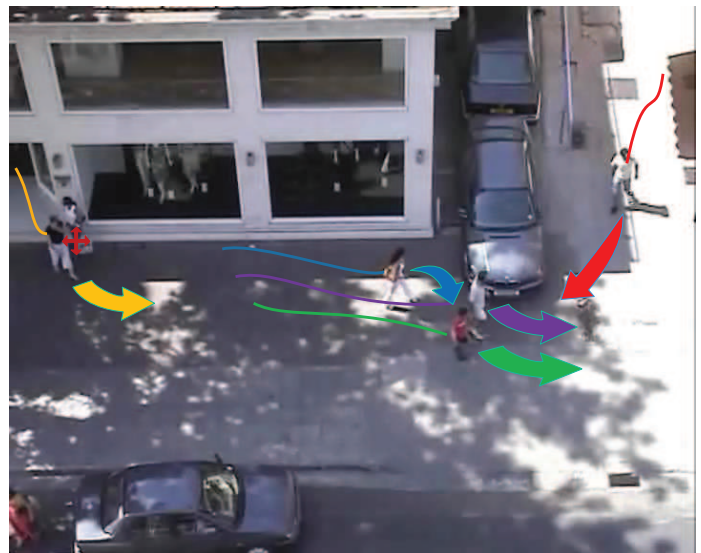


Fig. 1: Trajectory prediction. For two pedestrians in the scene, red trajectories are observed, and the task is to predict their future trajectories. Humans can easily do such an estimation. However, intelligent machines, such as robots, cannot easily do so (best viewed in color).

Early works related to trajectory prediction always depend on simple motion models, such as constant velocity and acceleration models. Thus, trajectory prediction could not be performed in complex scenes. Later, researchers utilize several stochastic models (e.g., Gaussian mixture regression [4] or dynamic Bayesian networks (DBNs) [5]) to model complex motions. However, such models need hand-crafted features, and thus are difficult to implement. Recent trends in deep learning, especially the recurrent neural network (RNN), provide a data-driven approach to understand complex motions. Specifically, the long-short term memory (LSTM) network is used to encode pedestrians’ motion patterns, and their future trajectories are estimated by sampling from the hidden states [6]. Recently, a social generative adversarial network (SGAN) is proposed to generate socially acceptable and multi-modal trajectories [7]. Except for the understanding of motion patterns, human—human interactions are modeled

B. Yang, G. Yan and Y. Chen are with the Department of Information Science and Engineering, Changzhou University, Changzhou, 213000 China.

P. Wang and C. Chan are with the California PATH, University of California, Berkeley, Richmond, CA, 94804, USA.

X. Liu is with the College of IoT Engineering, Hohai University, Changzhou, 213000, China.

Corresponding author: X. Liu (xfliu@hhu.edu.cn)

by a social pooling module on the basis of the common sense rules. Human—object interactions are captured by feeding the model with the scene- and object-level information through object detection and semantic segmentation. A detailed review is discussed in the next section.

Although remarkable progress has been made over the past years, two shortcomings that influence trajectory prediction performance remain. First, few works utilize the correlation between pedestrians’ head orientations and their future trajectories. A common sense is that a pedestrian’s future trajectory is always influenced by pedestrians in front. Utilizing such common sense is beneficial to model pedestrians’ social interactions. Second, few studies explore the latent variable, which plays a critical role in generating multi-modal predictions. Most works use random Gaussian noise as the latent variable. However, such a latent variable encompasses little knowledge about the scene or pedestrians and thus is not a good choice for an improved trajectory prediction.

In this work, we propose *Trajectory Predictor with Pseudo Oracle (TPPO)*, which adversarially trains a generator and discriminator. The generator contains an LSTM-based encoder-decoder and the discriminator contains an LSTM-based encoder. As indicated by Hasan et al. [8], pedestrians’ head orientations can be used as an oracle for an improved trajectory prediction. We propose to use pedestrians’ moving directions as a pseudo oracle, which approximately reflects their head orientations. Then, we utilize the correlation between pedestrians’ moving directions and their future trajectories through an attention mechanism. Such a mechanism highlights the influences among correlated pedestrians and thus can better model pedestrians’ social interactions. Besides, the latent variable distribution of ground-truth trajectories can be regarded as another oracle. We propose a novel latent variable predictor, which estimates two latent variable distributions from observed and ground-truth trajectories, respectively. Then, their Kullback-Leibler divergence (KL-divergence) is minimized during training. In the testing stage, the predictor estimates the latent variable distribution of observed trajectories. Such a distribution is similar to that of ground-truth trajectories, and thus can be regarded as another pseudo oracle. Pedestrians’ positions, velocities, and accelerations are extracted from their trajectories and then are fed into the latent variable predictor. Positions reflect the potential scene layout, whereas velocities and accelerations represent pedestrians’ motion patterns and radicalness. Notably, the proposed latent variable predictor learns knowledge from trajectories only, and thus increases little computational overhead.

Generally, our contributions are three-fold. (1) We propose a social attention pooling module that fully utilizes the correlation between pedestrians’ moving directions and their future trajectories. The attention mechanism improves the modeled social interactions. (2) We propose a novel latent variable predictor that can estimate a knowledge-rich latent variable for an improved prediction performance. Such a latent variable is learned from trajectories, and thus increase little computational overhead. (3) We embed the social attention pooling module and the latent variable predictor into a GAN framework to generate socially acceptable and multi-modal

outputs. Moreover, we achieve state-of-the-art performance on several trajectory forecasting benchmarks, including ETH [9] and UCY [10] datasets.

The rest of the paper is organized as follows. Section II reviews related works. Section III describes the proposed method in detail. Section IV presents the experimental results. Section V provides the conclusion and discussion.

II. RELATED WORK

A. Trajectory prediction methods

Trajectory prediction is a modeling problem that attempts to understand pedestrians’ motion patterns by examining pedestrian time-series data. Early works often focus on predicting future trajectories with dynamics-based methods, including constant velocity and acceleration models [11]. However, a simple kinematic model is unsuitable for long-term predictions. For long prediction horizons, flow-based methods [12][13] are proposed to learn the directional flow from observed trajectories in the scene. Subsequently, trajectories are generated by recursively sampling the distribution of future motion derived from the learned directional flow. To cope with complicated scenarios, researchers have resorted to several learning-based methods, such as Gaussian mixture regression [4], Gaussian process [14], random tree searching [15], hidden Markov models [16], and DBNs [5]. However, it is nontrivial to handle high-dimensional data with such traditional methods.

With the rise of deep learning, RNN provides a data-driven manner to encode pedestrians’ motion series. Prediction models have two kinds, namely, deterministic and generative models. For deterministic models, the distribution of future trajectories is estimated from the hidden state which is encoded by an LSTM or a gated recurrent unit (GRU). Alahi et al. [6] presented Social-LSTM, which models pedestrian motions with a shared LSTM and then performs trajectory prediction through sampling. Zhang et al. [17] proposed SR-LSTM, which recursively refines the hidden states of LSTM, to recognize the important current intention of neighbors. Improved prediction performance is guaranteed by refined hidden states. Certain works attempt to embed additional information. Xue et al. [18] and Syed et al. [19] utilized three LSTMs to encode person, social, and scene scale information and then aggregate them for context-aware trajectory prediction. Ridel et al. [20] presented a joint representation of the scene and past trajectories by using Conv-LSTM and LSTM, respectively. Lisotto et al. [21] improved Social-LSTM by encompassing prior knowledge about the scene as a navigation map that embodies most frequently crossed areas. Moreover, the scene context is obtained through semantic segmentation to restrain motion for additional plausible paths. These methods improve the prediction performance of Social-LSTM. However, they suffer from future uncertainties, which pose a great challenge in trajectory prediction.

Generative models handle future uncertainties by introducing an alterable latent variable. Lee et al. [22] presented DESIRE, which generates multi-modal predictions with conditional variational auto-encoders. Later, Gupta et al. [7] proposed SGAN, which adversarially trains the generator

and discriminator to produce socially acceptable trajectories. SGAN used the random Gaussian noise as the latent variable, and thus generated diverse outputs. Zhu et al [23] proposed StarNet, which is similar to SGAN except for the use of a query module. Amirian et al. [24] replaced the L2 loss used in SGAN with the information loss [25] to avoid mode collapse.

Besides methods mentioned above, reinforcement learning-based trajectory predictors [26][27][28][29][30] exhibit a rising trend. However, reinforcement learning-based methods always provide the optimal trajectory, whereas the true trajectory is sub-optimal due to pedestrians' randomness. Moreover, estimating pedestrians' destinations that are essential for reinforcement learning is difficult due to future uncertainties.

B. Social interaction modeling

Great efforts in trajectory prediction are devoted to modeling pedestrians' social interactions. These interactions can be defined by hand-crafted rules, such as social forces [31] and stationary crowds' influences [32]. However, capturing complex interactions in the scene with these rules is difficult. Therefore, current works always learn social interactions in a data-driven manner. Social-LSTM [6] first proposed the social pooling layer to aggregate neighbors' information in a certain grid. Pei et al. [32] proposed a social-affinity map by replacing the grid with a bin. SGAN [7] removed the regional restraint and directly aggregated all neighbors' information in the scene. To further capture pedestrians' social interactions, Amirian et al. [24] replaced the relative displacement with the bearing angle, the Euclidean distance, and the closest distance between the target person and neighbors. These additional variables calculated from observed trajectories are more intuitional in modeling social interactions than relative displacement. They also used an attention mechanism, which is effective in highlighting key neighbors and features as proposed in SoPhie [33].

Except for the social pooling layer and its variants, graph neural network is another mainstream to model pedestrians' social interactions [34] [35]. Such methods are especially good for handling heterogeneous agents [36] or crowd scenarios [37]. However, both methods neglect the correlation between pedestrian's head orientation and trajectory prediction. As reported by Hasan et al. [8], knowing the head orientation is beneficial for modeling social interactions. Specifically, future trajectories of the target person are influenced by pedestrians in front. However, such an oracle cue is difficult to estimate from image data. In this work, we approximately take pedestrians' moving directions as their head orientations and model their social interactions with a social attention pooling module.

C. Latent variable learning

Generative model-based prediction methods have gone mainstream due to their ability to handle future uncertainties. The latent variable used in the generator has a strong correlation with generated multi-modal outputs. Several previous works [7][33] used the random Gaussian noise as the latent variable and thus injected little knowledge about pedestrians or scenes into the generator. Amirian et al. [24] sampled part of

the latent variable from a uniform distribution on the interval from 0 to 1. However, associating the trajectory or the scene with a certain latent variable remains difficult. Zhang et al. [38] presented a stochastic module to generate the latent variable on the basis of pedestrians' movements. The latent variable is sampled from the embedding outputs of a social graph network. Tang et al. [39] proposed a dynamic encoder to learn latent variables from multiple inputs, including trajectories and the environmental context. However, processing the visual context needs more computation than processing trajectory data alone.

In this work, we propose a novel predictor that only learns the latent variable from trajectory data. Specifically, we feed pedestrians' positions, velocities, and accelerations into the predictor to learn the latent environmental context, pedestrians' motion patterns and radicalness. Unlike References [38] [39] that only utilized observed data, we attempt to minimize the latent variable distribution gaps between observed and ground-truth trajectories. Our inspiration comes from Reference [40], which focused on stochastic video generation with a learned prior.

III. PROPOSED METHOD

In this work, we develop a trajectory predictor that can generate multiple future trajectories of all agents in a scene with high accuracy. Fig. 2 illustrates the system pipeline of TPPO.

A. Problem definition

The trajectory prediction problem is a time-series analysis. For pedestrian i , we first denote his position (x_i^t, y_i^t) at time step t as p_i^t . The goal of trajectory prediction is to estimate his future trajectory $\mathcal{T}_i = (p_i^{t+1}, \dots, p_i^{t+T_{obs}})$, considering his motion history $\mathcal{H}_i = (p_i^0, \dots, p_i^t)$ and interactions with other pedestrians or objects. Then, the trajectory prediction problem is converted into a problem of finding a parametric model that predicts future trajectory \mathcal{T}_i , which can be formulated as follows:

$$\arg \max_{\Theta} P_{\theta}(\mathcal{T}_i | \mathcal{H}_0, \dots, \mathcal{H}_n), \quad (1)$$

where Θ represents learnable parameters, and n represents the number of pedestrians. Recently, the above-mentioned formulation is always converted into a sequence-to-sequence prediction problem, which can be addressed by the data-driven RNN module.

B. Generator and discriminator

As reviewed above, generative model-based methods are always used for trajectory prediction due to its ability in generating multi-modal outputs. Therefore, we design the structure of TPPO on the basis of SGAN, which can produce multi-modal and socially acceptable trajectories through adversarial training. We briefly introduce the generator and the discriminator as follows:

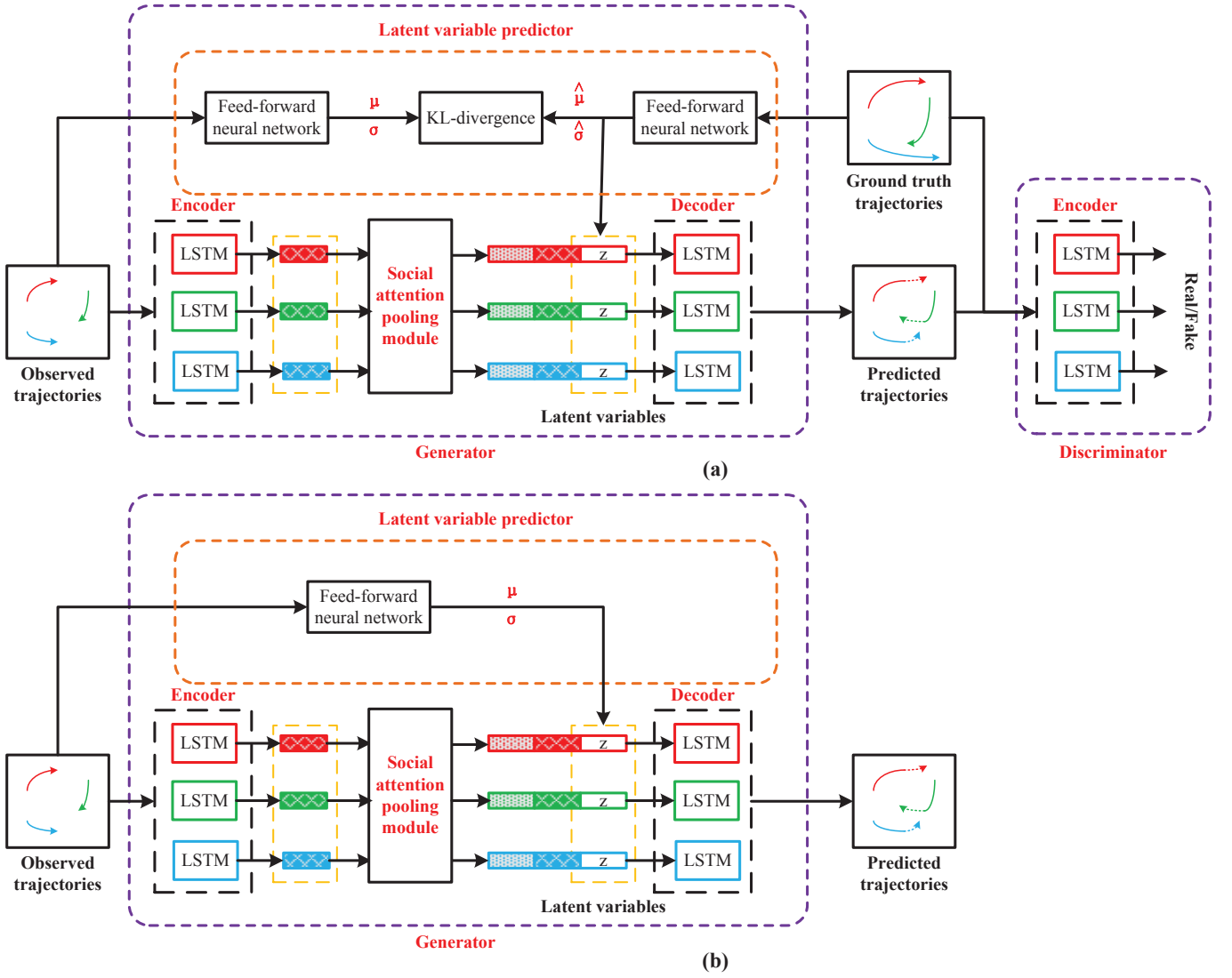


Fig. 2: System pipeline. Our model contains three key components: a generator, a discriminator, and a latent variable predictor. In the (a) training stage, the generator and discriminator are trained in an adversarial manner. The generator first encodes the input trajectories with an LSTM-based encoder, and then interactions are calculated by the social attention pooling module. Outputs of the encoder and pooling module are concatenated together with the latent variable estimated from ground-truth trajectories. These outputs are then decoded by an LSTM-based decoder to predict trajectories. The discriminator takes the input ground-truth and predicted trajectories and classifies them as socially acceptable or not. In the (b) testing stage, only the generator is reserved, and the latent variable is estimated from observed trajectories (best viewed in color).

Generator: The generator consists of a shared encoder-decoder and a social attention pooling module used to calculate pedestrians’ social interactions. A single layer MLP is used to convert the motion history of pedestrian i into a fixed-length vector e_i^t . Then, the vector is fed into an LSTM-based encoder to generate the hidden state of pedestrian i at time t as follows:

$$\begin{aligned} e_i^t &= \phi(x_i^t, y_i^t; W_{ee}) \\ h_{ei}^t &= LSTM(h_{ei}^{t-1}, e_i^t; W_{encoder}), \end{aligned} \quad (2)$$

where $\phi(\cdot)$ is a MLP function with ReLU nonlinearity. W_{ee} and $W_{encoder}$ are the learnable weights of $\phi(\cdot)$ and the encoder function $LSTM(\cdot)$, respectively.

Afterwards, pedestrians’ interactions are aggregated by the social attention pooling module and latent variables are esti-

mated by the latent variable predictor. We will discuss these two modules in detail later. Then, an LSTM-based decoder is used to estimate the future trajectories of pedestrian i on the basis of the concatenation of hidden state h_{ei}^t , pooling output P_i^t , and estimated latent variable z_i^t . The decoding is formulated as follows:

$$\begin{aligned} h_{di}^t &= LSTM(h_{di}^{t-1}, [h_{ei}^t, P_i^t, z_i^t]; W_{decoder}) \\ (\hat{x}_i^t, \hat{y}_i^t) &= \gamma(h_{di}^t) \end{aligned}, \quad (3)$$

where $\gamma(\cdot)$ is an MLP function with ReLU nonlinearity to predict future trajectories $(\hat{x}_i^t, \hat{y}_i^t)$. $W_{decoder}$ represents the learnable weight of the decoder, which is shared by all pedestrians in the scene.

Discriminator: The discriminator is used to classify the

predicted and ground-truth trajectories as socially acceptable or not. Both trajectories are fed into an LSTM-based encoder to generate the embedding, and then a Softmax classifier is used to perform classification on the basis of the embedding. Pedestrians' interactions are not needed in the discriminator.

C. Social attention pooling module

The social pooling layer proposed in SGAN can aggregate pedestrians' interactions in crowded scenes. However, such a pooling layer only considers relative positions between target people and their neighbors. As a common knowledge, pedestrians' future trajectories are always influenced by people in front. As demonstrated in Fig. 3, future trajectories of target A are influenced by targets B and C who are in A's field of view (FoV). Target D does not interfere A's trajectory decision even when he runs to A. Several previous works utilized pedestrians' head orientations to infer the FoV [8]. However, accurately recognizing pedestrians' head orientations from vision data is hard. Thus, utilizing such a common knowledge for an improved trajectory prediction is difficult.

TPPO uses an attention mechanism to utilize the correlation between pedestrians' head orientations and their trajectories. We approximately take pedestrians' moving directions at the last step as their head orientations. Then, the cosine values of all pedestrians' bearing angles are calculated as follows:

$$\cos(\mathcal{B}) = \begin{bmatrix} \cos(b_{11}) & \cdots & \cos(b_{1n}) \\ \vdots & \ddots & \vdots \\ \cos(b_{n1}) & \cdots & \cos(b_{nn}) \end{bmatrix}, \quad (4)$$

where n is the number of pedestrians in a scene. b_{ij} represents the bearing angle of agent j from agent i , that is, the angle between the velocity of agent i and the vector joining agents i and j .

Afterwards, the attentional weights are calculated on the basis of the cosine values. We perform hard and soft attention operations to refine the outputs of the second MLP module. Finally, outputs of the attention module are max-pooled to generate pedestrian A's pooling vector P_A . The hard and soft attention operations are formulated as follows:

Hard attention: As discussed above, the influence of one pedestrian on another decreases with the bearing angle increases. Therefore, hard attention weight is represented as a matrix H_A of the same size of $\cos(\mathcal{B})$, and each element h_{ij} in H_A is set to 0 or 1 by thresholding. h_{ij} is set to 1 if $\cos(b_{ij})$ is larger than an empirically threshold -0.2 , otherwise is set to 0.

Soft attention: Unlike hard attention that calculates attention weight by thresholding, soft attention adaptively calculates the correlations of various pedestrian pairs. Soft attention weight S_A can be formulated as follows:

$$S_A = \delta(\varphi(\cos(\mathcal{B}))), \quad (5)$$

where $\delta(\cdot)$ represents the sigmoid activation, and $\varphi(\cdot)$ represents the 1×1 convolution.

D. Latent variable predictor

The latent variable predictor is used to estimate an alterable latent variable for generating multi-modal outputs. Specifically, we attempt to train a well-learned predictor, which can estimate similar latent variable distributions from observed and ground-truth trajectories, respectively. Afterwards, the predictor can estimate knowledge-rich latent variables from observed trajectories only in the testing stage. Inputs to the latent variable predictor are pedestrians' positions, velocities, and accelerations of trajectories. As shown in Fig. 2, the latent variable predictor consists of two feed-forward neural networks, which are formulated as follows:

$$\begin{aligned} (\mu_i^k, \sigma_i^k) &= \Psi(I_i^k; W_{LP}^k) \\ (\hat{\mu}_i^k, \hat{\sigma}_i^k) &= \hat{\Psi}(\hat{I}_i^k; \hat{W}_{LP}^k) \end{aligned}, \quad (6)$$

where $\Psi(\cdot)$ and $\hat{\Psi}(\cdot)$ are the feed-forward neural networks with learnable weights W_{LP}^k and \hat{W}_{LP}^k , respectively. I_i^k and \hat{I}_i^k are the k^{th} kinds of inputs (positions, velocities, and accelerations) we extract from observed and ground-truth trajectories, respectively. (μ_i^k, σ_i^k) and $(\hat{\mu}_i^k, \hat{\sigma}_i^k)$ represent the latent variable distributions of the k^{th} kind of input estimated by $\Psi(\cdot)$ and $\hat{\Psi}(\cdot)$, respectively. Final latent variable z is generated by concatenating the latent variable distributions of three kinds of inputs and the random Gaussian noise. $(\hat{\mu}_i^k, \hat{\sigma}_i^k)$ and (μ_i^k, σ_i^k) are used in the training and testing stages, respectively. The random Gaussian noise is used to generate multi-modal outputs as that used in SGAN. The latent variable estimated by the proposed predictor is expected to provide rich information for accurate trajectory prediction while maintaining the ability to handle future uncertainties.

E. Loss function

The loss function used in this work consists of three parts: adversarial, variety, and latent variable distribution losses. The adversarial loss is used to generate socially acceptable trajectories by performing a two-player min-max game. Unlike traditional GAN, the latent variable z used in this work is sampled from the ground-truth trajectory at the training stage with the latent variable predictor. Thus, the adversarial loss is formulated as follows:

$$\begin{aligned} \mathcal{L}_{adv} &= \\ &\mathbb{E}_{x \sim p_{data}(x)} [\log D(x)] + \mathbb{E}_{z \sim p(z|\hat{I}_i^k)} [\log(1 - D(G(z|\hat{I}_i^k)))] \end{aligned}, \quad (7)$$

The variety loss is used to fit the best-predicted trajectory in L2 loss while maintaining multi-modal outputs. We follow its definition proposed in SGAN and the variety loss is defined as follows:

$$\mathcal{L}_{variety} = \min_m \left\| \hat{\mathcal{T}}_i - \mathcal{T}_i^m \right\|_2, \quad (8)$$

where $\hat{\mathcal{T}}_i$ and \mathcal{T}_i^m are ground-truth and the m^{th} predicted trajectories, respectively. m is a hyper-parameter and is set to 20 according to SGAN.

The latent variable distribution loss is used to measure the latent variable distribution gaps between observed and ground-

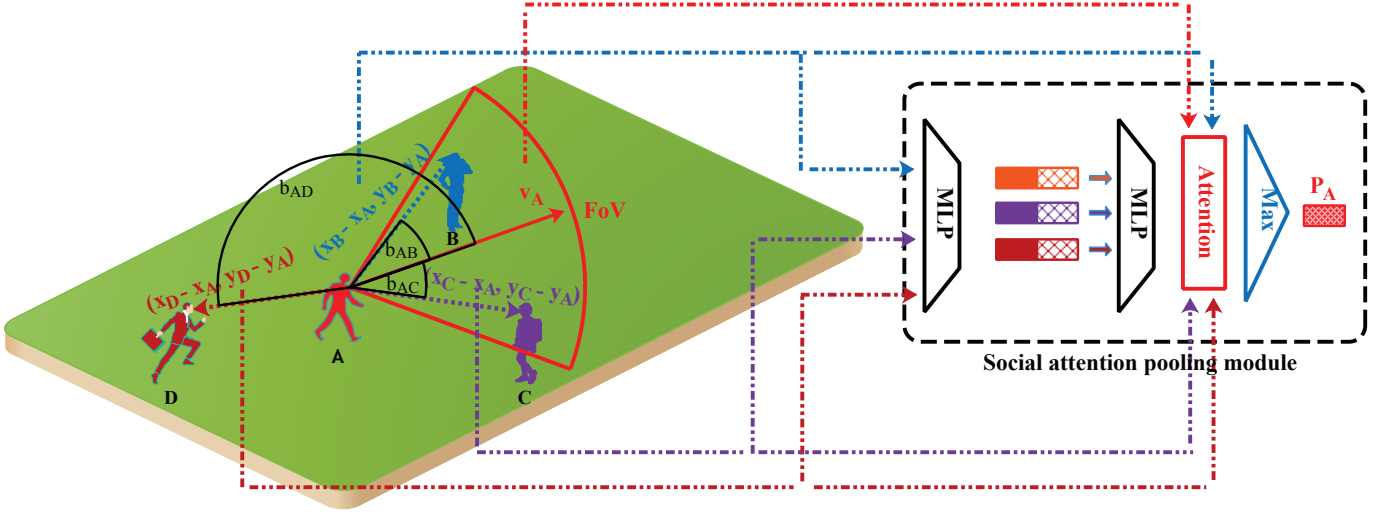


Fig. 3: Social attention pooling module. Compared with the social pooling layer proposed in SGAN, we add an attention module with the soft or hard operation. The left part illustrates the social effects between pedestrian A and his neighbors. FoV is defined on the basis of A’s velocity V_A . Intuitively, pedestrians B and C in the FoV can influence A’s future trajectories, whereas D contributes little to A’s trajectory prediction. The right part demonstrates the pipeline of information pooling. Outputs of the second MLP are weighted by the attention mechanism, and then are pooled element-wise to compute A’s pooling vector V_A . The proposed social attention pooling module can model interactions between all pairs of pedestrians (best viewed in color).

truth trajectories. We utilize KL-divergence to calculate the loss, which is formulated as follows:

$$\mathcal{L}_{LD} = D_{KL}((\mu_i^k, \sigma_i^k) || (\hat{\mu}_i^k, \hat{\sigma}_i^k)), \quad (9)$$

Afterwards, the total loss is defined in a weighted manner as follows:

$$\mathcal{L}_{total} = \mathcal{L}_{adv} + \alpha \times \mathcal{L}_{variety} + \beta \times \mathcal{L}_{LD}, \quad (10)$$

where α and β are set to 1 and 10 respectively by cross validation across benchmarking datasets.

F. Implementation details

LSTMs are used as the RNN for encoder and decoder, in which the dimensions of the hidden states are 32. Each element in velocities, positions, and accelerations are embedded as 16-dimensional vectors. The eight-dimensional latent variable z contains three two-dimensional vectors that embedded from positions, velocities, and accelerations and another two-dimensional random Gaussian noise. We iteratively train the generator and discriminator with a batch size of 64 for 600 epochs using Adam [41], with the initial learning rate of 0.001. The training frequency of the discriminator is twice as that of the generator for better convergence. The proposed model is built with a Pytorch framework and is trained with an NVIDIA GTX-1080 GPU.

IV. EXPERIMENTAL RESULTS

The proposed method is evaluated on two publicly available datasets, namely ETH [9] and UCY [10]. Both of them consist of real-world pedestrian trajectories with rich human-human and human-object interaction scenarios. There are five sets of

data, namely ETH, HOTEL, UNIV, ZARA1, and ZARA2. In total there are 1,536 pedestrians in challenging scenarios such as people crossing each other, group forming and dispersing, and collision avoidance. All the trajectories are converted to real-world coordinates, which are sampled every 0.4 seconds through the interpolation operation.

Similar to several prior works [7][24], the proposed method is evaluated with two error metrics as follows:

1. *Average Displacement Error (ADE)*: Average L2 distance between the ground-truth trajectory and the predicted trajectory over all predicted time steps.
2. *Final Displacement Error (FDE)*: The Euclidean distance between the true final destination and the predicted final destination at the last step of prediction.

We use the leave-one-out approach similar to that adopted by Social-LSTM [6]. Specifically, we train models on four sets and test them on the remaining set. The observed and predicted horizons are 8 (3.2 seconds) and 8 / 12 (3.2 / 4.8 seconds) time steps, respectively. We denote T as the prediction horizon.

A. Quantitative evaluations

Comparisons with baseline methods: We compare the proposed method against the following baselines:

1. *Linear*: A linear regressor is used to predict future trajectories by minimizing the least square error.
2. *LSTM*: An LSTM is used to embed the motion patterns of observed trajectories. Future trajectories are predicted on the basis of the learned motion patterns.
3. *Social-LSTM* [6]: An improved LSTM-based trajectory prediction method by proposing a social pooling layer to aggregate hidden states of interested pedestrians. Future trajec-

tories are predicted by decoding the concatenation of LSTM embedding and social pooling outputs.

4. *SGAN* [7]: An improved version of Social-LSTM by utilizing adversarial training to generate socially acceptable trajectories. Gaussian noises are used as latent variables to generate multi-modal outputs in consideration of pedestrians’ future uncertainties. The model is trained using a variety loss with the hyper-parameter set to 20. During the test, 20 times are sampled from the generator and the best prediction in L2 sense is used for quantitative evaluation.

Table 1 lists the quantitative results between TPPO, with either soft or hard attention modules, and the abovementioned baseline methods across five datasets. TPPO with hard attention module outperforms all baseline methods in ADE and FDE for both prediction horizons.

Comparisons with state-of-the-art methods: We compare the proposed method against the following state-of-the-art methods:

1. *SR-LSTM* [17]: An improved version of Social-LSTM by proposing a data-driven state refinement module. Such a module iteratively refines the current pedestrians’ hidden states on the basis of their neighbors’ intentions through message passing.

2. *Sophie* [33]: An improved version of SGAN by utilizing attention mechanisms, namely, the social and physical attention modules. The trajectory prediction performance is improved by highlighting the key information with attention operations.

3. *S-Way* [24]: An improved version of SGAN by replacing the L2-loss with the information-loss proposed in Reference [25] to avoid mode collapsing.

4. *Social-BiGAT* [34]: An improved version of SGAN by using the bicycle structure to train the generator. A graph attention network is used to model social interactions for better prediction performance.

5. *STGAT* [35]: An auto-encoder based trajectory prediction method that uses a spatio-temporal graph attention network to model pedestrians’ social interactions in the scene. Specifically, the spatial interactions are captured by the graph attention mechanism, and temporal correlations are modeled by a shared LSTM.

Table 2 presents the comparison between TPPO and state-of-the-art methods. Similar to results in Table 1, TPPO with hard attention module almost outperforms others in both prediction horizons in UNIV, ZARA1, and ZARA2 datasets. S-Ways performs well in ETH and HOTEL datasets by designing an attention-based module that focuses on the bearing angle, the Euclidean distance, and the distance of the closest approach. Such a module can capture human-human and human-object interactions in complex scenes that contain lots of obstacles. However, S-Ways performs poorly in ZARA1 and ZARA2 datasets. STGAT achieves the sub-optimal average ADE and FDE because of the usage of the spatio-temporal graph attention network. It reveals the fact that the graph model is good at capturing social interactions which are significant for accurate trajectory prediction. The spatio-temporal mechanism used in STGAT makes it better than Social-BiGAT that also uses a graph attention network to

capture social interactions. Compared with the state-of-the-art methods, our method achieves the best performance in average ADE and FDE values. Moreover, the hard attention module performs better than the soft attention module.

B. Ablation study

We conduct an ablation study to demonstrate the effects of various modules used in TPPO. Soft and Hard represent soft and hard attention modules, respectively. The MLP module represents the latent variable predictor with multiple inputs. For comparison, we propose the SLP module, which uses the velocity only to estimate the latent variable. As presented in Table 3, the SLP module does not improve the prediction performance of SGAN. However, the MLP module drastically decreases the ADE and FDE errors in most datasets compared with SGAN. Such findings confirm the effectiveness of multiple inputs in latent variable prediction. Besides, we embed hard and soft attention modules into SGAN to evaluate the effectiveness of the social attention pooling layer. For SGAN, the soft attention module is slightly better than the hard attention module, whereas an opposite conclusion is drawn when both attention modules are used in TPPO. The possible reason for such slight nonconformity is the differences in network structures. Specifically, TPPO makes a trade-off between the learning of the soft attention module and latent variable predictor, whereas SGAN only focuses on the soft attention module during training.

C. Evaluations of different sampling times

Despite the necessity of generating multi-modal outputs, a good trajectory predictor should estimate accurate future trajectories with few attempts. One advantage of TPPO is its ability to forecast accurate trajectories with few attempts. We perform a comparison between SGAN and TPPO with the MLP module only with gradually decreasing sampling times. Fig. 6 illustrates the comparison results of ADE and FDE between TPPO and SGAN when using different sampling times across five datasets. Except for the ADE and FDE for $T = 12$ in the HOTEL dataset, TPPO greatly outperforms SGAN, especially with few sampling times. We can observe that the ADE and FDE values of TPPO gently increase while sampling times are decreasing. However, those of SGAN drastically increase when the number of samples is close to 1. The difference indicates the power of TPPO in predicting accurate future trajectories with few attempts.

D. Qualitative evaluations

TPPO performs accurate trajectory prediction on the basis of the latent variable predictor, which only estimates a knowledge-rich latent variable from the trajectory data. Fig. 4 demonstrates the trajectory prediction results by using SGAN, SR-LSTM, Sophie, and TPPO with different modules in different datasets. Specifically, we show the prediction results of TPPO with the MLP module only, with MLP and soft attention modules, and with MLP and hard attention modules. Each sub-figure represents a scene with multiple

TABLE I: Quantitative results between the proposed method and baseline methods mentioned above across five datasets. We report the ADE and FDE for $T = 8$ and $T = 12$ (8 / 12) in meters. Our method outperforms almost all baseline methods (low is preferred and is labeled with bold fonts).

| Metric | Dataset | Linear | LSTM | Social-LSTM [6] | SGAN [7] | TPPO | |
|--------|---------|-----------|-----------|-----------------|-----------|-------------------|------------------|
| | | | | | | + Soft | + Hard |
| ADE | ETH | 0.84/1.33 | 0.70/1.09 | 0.73/1.09 | 0.60/0.87 | 0.64/0.79 | 0.51/0.75 |
| | HOTEL | 0.35/0.39 | 0.55/0.86 | 0.49/0.79 | 0.52/0.67 | 0.28/0.37 | 0.22/0.36 |
| | UNIV | 0.56/0.82 | 0.36/0.61 | 0.41/0.67 | 0.44/0.76 | 0.28/0.48 | 0.25/0.39 |
| | ZARA1 | 0.41/0.62 | 0.25/0.41 | 0.27/0.47 | 0.22/0.35 | 0.14/ 0.22 | 0.13/0.22 |
| | ZARA2 | 0.53/0.77 | 0.31/0.52 | 0.33/0.56 | 0.29/0.42 | 0.12/ 0.18 | 0.11/0.23 |
| AVG | | 0.54/0.79 | 0.43/0.70 | 0.45/0.72 | 0.41/0.61 | 0.29/0.41 | 0.24/0.39 |
| FDE | ETH | 1.60/2.94 | 1.45/2.41 | 1.48/2.35 | 1.19/1.62 | 1.12/1.42 | 0.82/1.27 |
| | HOTEL | 0.60/0.72 | 1.17/1.91 | 1.01/1.76 | 1.02/1.37 | 0.46/ 0.70 | 0.35/0.70 |
| | UNIV | 1.01/1.59 | 0.77/1.31 | 0.84/1.40 | 0.84/1.52 | 0.54/0.94 | 0.46/0.74 |
| | ZARA1 | 0.74/1.21 | 0.53/0.88 | 0.56/1.00 | 0.43/0.68 | 0.24/0.39 | 0.21/0.37 |
| | ZARA2 | 0.95/1.48 | 0.65/1.11 | 0.70/1.17 | 0.58/0.84 | 0.20/ 0.31 | 0.18/0.45 |
| AVG | | 0.98/1.59 | 0.91/1.52 | 0.91/1.54 | 0.81/1.21 | 0.51/0.75 | 0.40/0.71 |

TABLE II: Comparison results with state-of-the-art methods across all datasets. We report the ADE and FDE for $T = 12$ in meters. Our method outperforms state-of-the-art methods in UNIV, ZARA1, and ZARA2 datasets, and is specifically good for average ADE and FDE (low is preferred and is labeled with bold fonts).

| Metric | Dataset | SR-LSTM | Sophie | S-Ways | Social-BiGAT | STGAT | TPPO | |
|--------|---------|---------|--------|-------------|--------------|-------------|-------------|-------------|
| | | | | | | | + Soft | + Hard |
| ADE | ETH | 0.63 | 0.70 | 0.39 | 0.69 | 0.65 | 0.79 | 0.75 |
| | HOTEL | 0.37 | 0.76 | 0.39 | 0.49 | 0.35 | 0.37 | 0.36 |
| | UNIV | 0.51 | 0.54 | 0.55 | 0.55 | 0.52 | 0.48 | 0.39 |
| | ZARA1 | 0.41 | 0.30 | 0.44 | 0.30 | 0.34 | 0.22 | 0.22 |
| | ZARA2 | 0.32 | 0.38 | 0.51 | 0.36 | 0.29 | 0.18 | 0.23 |
| AVG | | 0.45 | 0.54 | 0.46 | 0.48 | 0.43 | 0.41 | 0.39 |
| FDE | ETH | 1.25 | 1.43 | 0.64 | 1.29 | 1.12 | 1.42 | 1.27 |
| | HOTEL | 0.74 | 1.67 | 0.66 | 1.01 | 0.66 | 0.70 | 0.70 |
| | UNIV | 1.10 | 1.24 | 1.31 | 1.32 | 1.10 | 0.94 | 0.74 |
| | ZARA1 | 0.90 | 0.63 | 0.64 | 0.62 | 0.69 | 0.39 | 0.37 |
| | ZARA2 | 0.70 | 0.78 | 0.92 | 0.75 | 0.60 | 0.31 | 0.45 |
| AVG | | 0.94 | 1.15 | 0.83 | 1.00 | 0.83 | 0.75 | 0.71 |

pedestrians. For each pedestrian, the predicted trajectory is the best one with the lowest ADE value among the 20 samples generated by each method. Generally, all methods can predict future trajectories with high accuracy most of the time. Significantly, TPPO performs better than the selected state-of-the-art methods with predicted future trajectories closer to the ground-truth. Moreover, as illustrated in the fourth scenario of Fig. 4(c), TPPO can handle a sudden motion change, which is a challenging issue in trajectory prediction. Therefore, the information learned from positions, velocities, and accelerations is useful for accurate trajectory prediction in most cases. However, such information may mislead TPPO to generate wrong results in rare cases, as shown in the third scenario of Fig. 4(b). We will investigate the robustness of the latent variable predictor in our future work.

TPPO forecasts socially acceptable trajectories while maintaining diverse outputs by injecting the random Gaussian noise into the predicted latent variable. Fig. 5 illustrates the density maps of the predicted trajectories in four typical scenarios selected from different datasets. Density maps in the UNIV dataset are not shown because too many trajectories are present in each scene. In the first row, the MLP module helps TPPO to recognize the change of motion direction, whereas methods without the MLP module fail. In the second row, the MLP module helps TPPO to avoid the tree, and the attention module encourages the model to generate separate outputs, which are socially acceptable. The two scenarios in ZARA1 and ZARA2 datasets reveal the ability of TPPO in handling motion changes. The difference between these two scenarios is that the fourth row demonstrates a crowded scene. Therefore, the

TABLE III: Ablation study. We report the ADE and FDE for $T = 8$ and $T = 12$ (8 / 12) in meters across five datasets. SLP / MLP represent single / multiple inputs latent variable predictor, respectively. Soft / Hard represent soft and hard attention mechanisms, respectively (low is preferred and is labeled with bold fonts).

| Metric | Dataset | SGAN | + SLP | + MLP | + Soft | + Hard | + MLP + Soft | + MLP + Hard |
|--------|---------|-----------|-----------|-------------------|-----------|-----------|-------------------|------------------|
| ADE | ETH | 0.60/0.87 | 0.71/0.94 | 0.64/ 0.67 | 0.73/0.84 | 0.67/0.86 | 0.64/0.79 | 0.51/0.75 |
| | HOTEL | 0.52/0.67 | 0.42/0.65 | 0.29/0.44 | 0.36/0.49 | 0.50/0.51 | 0.28/0.37 | 0.22/0.36 |
| | UNIV | 0.44/0.76 | 0.40/0.70 | 0.27/0.45 | 0.38/0.63 | 0.39/0.62 | 0.28/0.48 | 0.25/0.39 |
| | ZARA1 | 0.22/0.35 | 0.23/0.40 | 0.17/0.24 | 0.21/0.32 | 0.21/0.34 | 0.14/ 0.22 | 0.13/0.22 |
| | ZARA2 | 0.29/0.42 | 0.21/0.34 | 0.13/0.21 | 0.20/0.29 | 0.20/0.29 | 0.12/ 0.18 | 0.11/0.23 |
| AVG | | 0.41/0.61 | 0.39/0.61 | 0.30/0.40 | 0.38/0.51 | 0.39/0.52 | 0.29/0.41 | 0.24/0.39 |
| FDE | ETH | 1.19/1.62 | 1.35/1.96 | 1.12/ 1.13 | 1.37/1.67 | 1.28/1.71 | 1.12/1.42 | 0.82/1.27 |
| | HOTEL | 1.02/1.37 | 0.81/1.40 | 0.58/0.91 | 0.68/0.98 | 0.96/1.08 | 0.46/ 0.70 | 0.35/0.70 |
| | UNIV | 0.84/1.52 | 0.83/1.49 | 0.51/ 0.69 | 0.79/1.34 | 0.81/1.34 | 0.54/0.94 | 0.46/0.74 |
| | ZARA1 | 0.43/0.68 | 0.46/0.82 | 0.30/0.42 | 0.41/0.64 | 0.40/0.68 | 0.24/0.39 | 0.21/0.37 |
| | ZARA2 | 0.58/0.84 | 0.43/0.73 | 0.22/0.36 | 0.40/0.60 | 0.40/0.61 | 0.20/ 0.31 | 0.18/0.45 |
| AVG | | 0.81/1.21 | 0.78/1.28 | 0.55/ 0.70 | 0.73/1.05 | 0.77/1.08 | 0.51/0.75 | 0.40/0.71 |

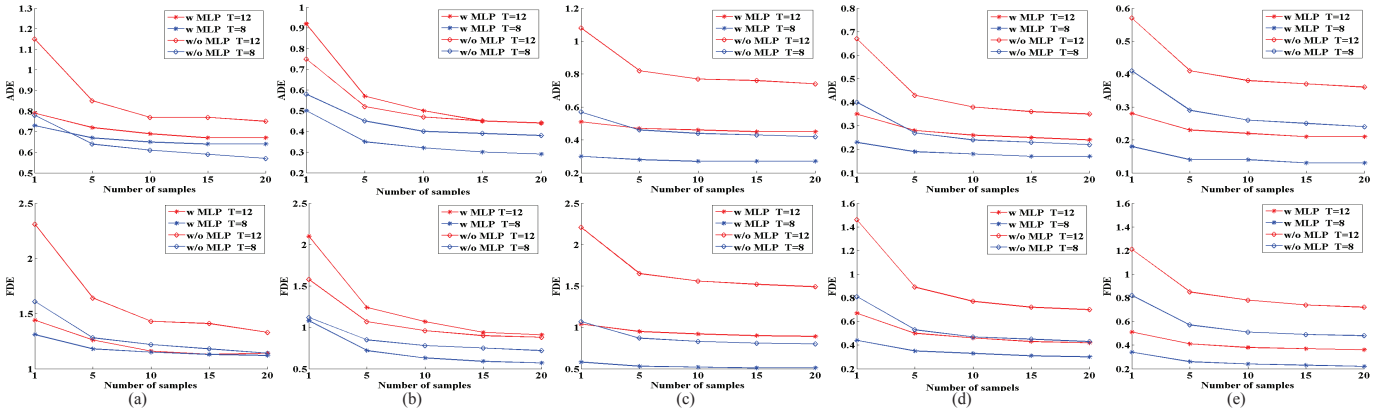


Fig. 4: Comparison results of ADE and FDE values between TPPO and SGAN when using different numbers of samples across (a) ETH, (b) HOTEL, (c) UNIV, (d) ZARA1, and (e) ZARA2 datasets. The upper and lower parts are comparison results of ADE and FDE, respectively. The star marker represents the proposed method, and the diamond marker represents SGAN. The red and blue lines (including the dashed) represent the prediction results for $T = 12$ and $T = 8$ in meters, respectively (best viewed in color and zoom-in.)

attention module can improve the prediction results compared with those of using the MLP module alone.

V. CONCLUSION AND DISCUSSION

In this work, we propose TPPO, which forecasts future trajectories with two pseudo oracles. One pseudo oracle is pedestrians' moving directions which are used to approximate pedestrians' head orientations. A social attention pooling module utilizes this pseudo oracle for an improved trajectory prediction performance. Another pseudo oracle is the latent variable distribution estimated from observed trajectories. We propose a novel latent variable predictor, which estimates the latent variable distribution from observed trajectories. Such a distribution is similar to that from ground-truth. The random Gaussian noise is injected into the estimated latent variable to handle future uncertainties. Evaluations are performed in two commonly used metrics, namely, ADE and FDE, across five benchmarking datasets. Comparisons with state-of-the-art approaches indicate the effectiveness of the proposed latent

variable predictor. Ablation studies reveal the necessity of learning information from multiple inputs and the superiority of accurate trajectory prediction with few sampling times. In addition, the proposed method only learns knowledge from trajectories and thus increases little computing overhead. Our future work focuses on how to control the latent variable for an improved prediction performance.

ACKNOWLEDGMENT

This work has been supported by the National key R&D program 2018AAA0100800, the Key Research and Development Program of Jiangsu under grants BE2017071, BE2017647 and BE2018004-04, the Natural Science Foundation of the Jiangsu Higher Education Institutions of China under Grant No. 18KJB520003, Key Laboratory for New Technology Application of Road Conveyance of Jiangsu Province under Grant BM20082061708, the Open Research Fund of State Key Laboratory of Bioelectronics, Southeast University under grant 2019005, and the State Key Laboratory

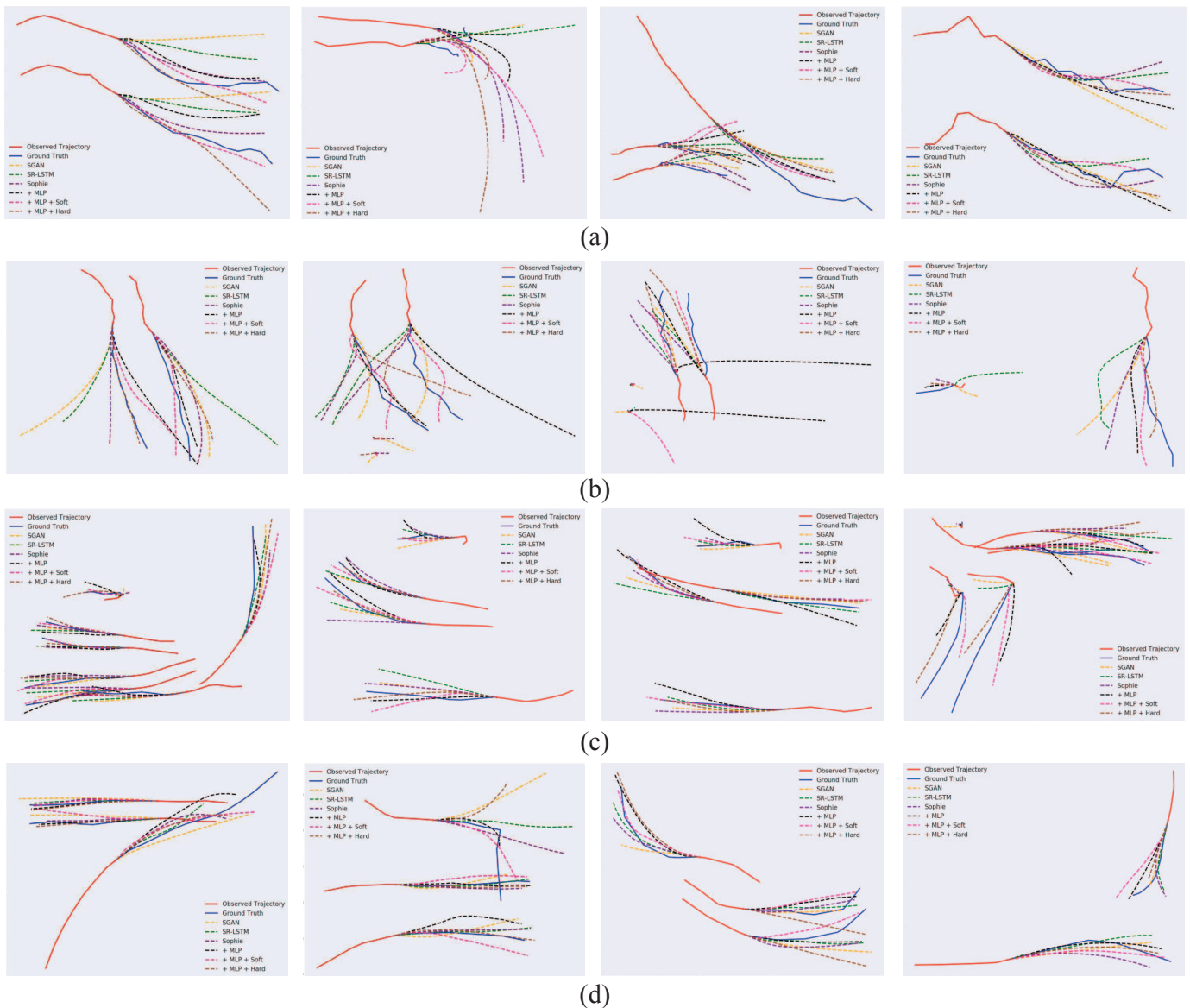


Fig. 5: Trajectory prediction results using SGAN, SR-LSTM, Sophie, and TPPO with different modules in (a) ETH, (b) HOTEL, (c) ZARA1, and (d) ZARA2 datasets. Red and blue lines represent observed and ground-truth trajectories, respectively. Dashed lines of different colors represent the predicted trajectories of different methods. We show the best trajectory with the lowest ADE value from 20 predicted samples (best viewed in color and zoom-in).

of Integrated Management of Pest Insects and Rodents under grant IPM1914, the China Academy of Railway Sciences Corporation Limited Foundation Project 2018YJ102.

REFERENCES

- [1] J. Hong, B. Sapp, and J. Philbin, “Rules of the road: Predicting driving behavior with a convolutional model of semantic interactions,” in *Proceedings of the IEEE Conference on Computer Vision and Pattern Recognition*, 2019, pp. 8454–8462.
- [2] M. Lubner, J. A. Stork, G. D. Tipaldi, and K. O. Arras, “People tracking with human motion predictions from social forces,” in *2010 IEEE International Conference on Robotics and Automation*. IEEE, 2010, pp. 464–469.
- [3] X.-H. Chen and J.-H. Lai, “Detecting abnormal crowd behaviors based on the div-curl characteristics of flow fields,” *Pattern Recognition*, vol. 88, pp. 342–355, 2019.
- [4] J. Li, W. Zhan, and M. Tomizuka, “Generic vehicle tracking framework capable of handling occlusions based on modified mixture particle filter,” in *2018 IEEE Intelligent Vehicles Symposium (IV)*. IEEE, 2018, pp. 936–942.
- [5] D. Kasper, G. Weidl, T. Dang, G. Breuel, A. Tamke, A. Wedel, and W. Rosenstiel, “Object-oriented bayesian networks for detection of lane change maneuvers,” *IEEE Intelligent Transportation Systems Magazine*, vol. 4, no. 3, pp. 19–31, 2012.
- [6] A. Alahi, K. Goel, V. Ramanathan, A. Robicquet, L. Fei-Fei, and S. Savarese, “Social lstm: Human trajectory prediction in crowded spaces,” in *Proceedings of the IEEE conference on computer vision and pattern recognition*, 2016, pp. 961–971.
- [7] A. Gupta, J. Johnson, L. Fei-Fei, S. Savarese, and A. Alahi, “Social gan: Socially acceptable trajectories with generative adversarial networks,” in *Proceedings of the IEEE Conference on Computer Vision and Pattern Recognition*, 2018, pp. 2255–2264.
- [8] I. Hasan, F. Setti, T. Tsesmelis, A. Del Bue, M. Cristani, and F. Galasso, “‘‘seeing is believing’’: Pedestrian trajectory forecasting using visual frustum of attention,” in *2018 IEEE Winter Conference on Applications*

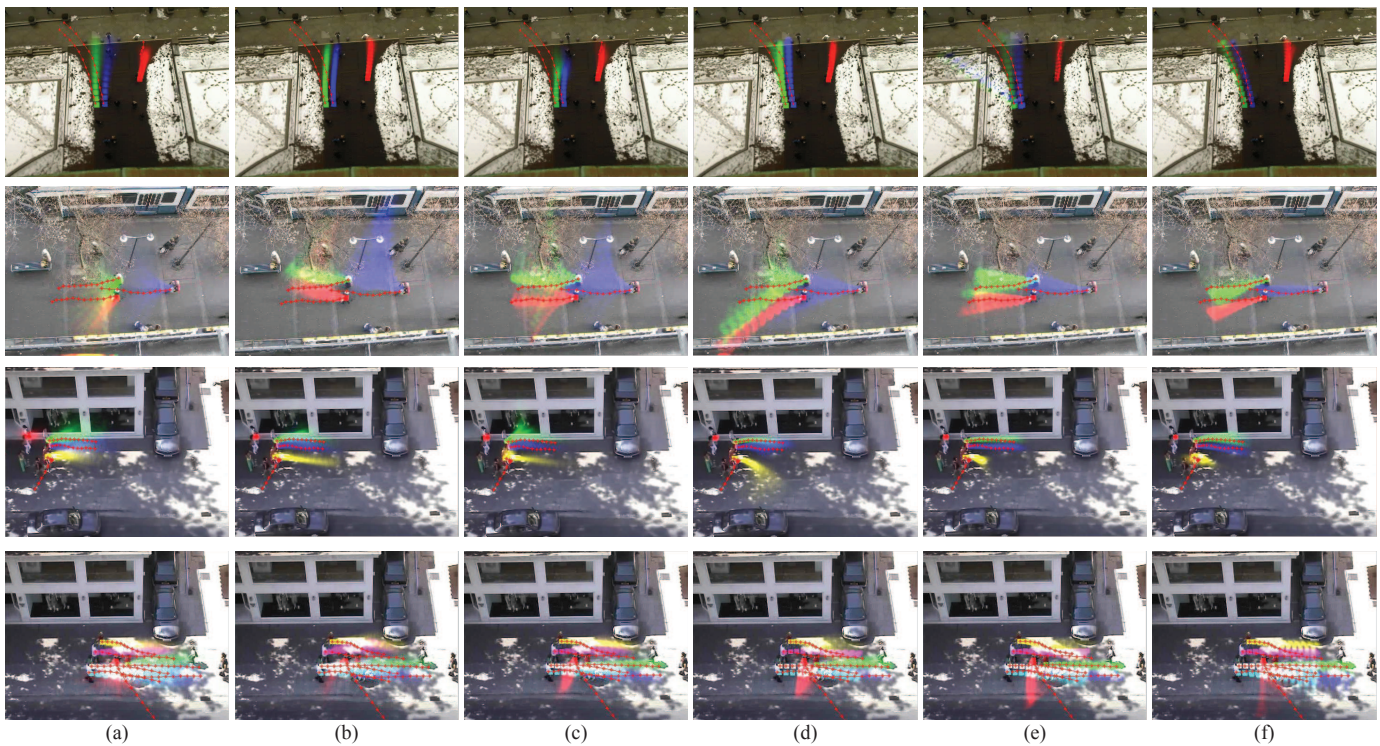


Fig. 6: Density maps of the predicted trajectories by using SGAN and TPPO with different modules, including (a) SGAN, (b) + Soft, (c) + Hard, (d) + MLP, (e) + MLP + Soft, and (f) + MLP + Hard. The first, second, third, and fourth rows are typical scenarios chosen from the ETH, HOTEL, ZARA1, and ZARA2 datasets, respectively. The density maps are generated by sampling 300 times from the learned generators. The red stars represent the true future trajectories, and different colors indicate the density distributions of different pedestrians (best viewed in color and zoom-in).

- of Computer Vision (WACV). IEEE, 2018, pp. 1178–1185.
- [9] S. Pellegrini, A. Ess, and L. Van Gool, “Improving data association by joint modeling of pedestrian trajectories and groupings,” in *European conference on computer vision*. Springer, 2010, pp. 452–465.
- [10] L. Leal-Taixé, M. Fenzi, A. Kuznetsova, B. Rosenhahn, and S. Savarese, “Learning an image-based motion context for multiple people tracking,” in *Proceedings of the IEEE Conference on Computer Vision and Pattern Recognition*, 2014, pp. 3542–3549.
- [11] S. Zernetsch, S. Kohnen, M. Goldhammer, K. Doll, and B. Sick, “Trajectory prediction of cyclists using a physical model and an artificial neural network,” in *2016 IEEE Intelligent Vehicles Symposium (IV)*. IEEE, 2016, pp. 833–838.
- [12] W. Zhi, R. Senanayake, L. Ott, and F. Ramos, “Spatiotemporal learning of directional uncertainty in urban environments with kernel recurrent mixture density networks,” *IEEE Robotics and Automation Letters*, vol. 4, no. 4, pp. 4306–4313, 2019.
- [13] S. Molina, G. Cielniak, T. Krajník, and T. Duckett, “Modelling and predicting rhythmic flow patterns in dynamic environments,” in *Annual Conference Towards Autonomous Robotic Systems*. Springer, 2018, pp. 135–146.
- [14] C. Laugier, I. E. Paromtchik, M. Perrollaz, M. Yong, J.-D. Yoder, C. Tay, K. Mekhnacha, and A. Nègre, “Probabilistic analysis of dynamic scenes and collision risks assessment to improve driving safety,” *IEEE Intelligent Transportation Systems Magazine*, vol. 3, no. 4, pp. 4–19, 2011.
- [15] G. Aoude, J. Joseph, N. Roy, and J. How, “Mobile agent trajectory prediction using bayesian nonparametric reachability trees,” in *Infotech@ Aerospace 2011*, 2011, p. 1512.
- [16] W. Wang, J. Xi, and D. Zhao, “Learning and inferring a driver’s braking action in car-following scenarios,” *IEEE Transactions on Vehicular Technology*, vol. 67, no. 5, pp. 3887–3899, 2018.
- [17] P. Zhang, W. Ouyang, P. Zhang, J. Xue, and N. Zheng, “Sr-lstm: State refinement for lstm towards pedestrian trajectory prediction,” in *Proceedings of the IEEE Conference on Computer Vision and Pattern Recognition*, 2019, pp. 12085–12094.
- [18] H. Xue, D. Q. Huynh, and M. Reynolds, “Ss-lstm: A hierarchical lstm model for pedestrian trajectory prediction,” in *2018 IEEE Winter Conference on Applications of Computer Vision (WACV)*. IEEE, 2018, pp. 1186–1194.
- [19] A. Syed and B. T. Morris, “Sseg-lstm: Semantic scene segmentation for trajectory prediction,” in *2019 IEEE Intelligent Vehicles Symposium (IV)*. IEEE, 2019, pp. 2504–2509.
- [20] D. Ridel, N. Deo, D. Wolf, and M. Trivedi, “Scene compliant trajectory forecast with agent-centric spatio-temporal grids,” *arXiv preprint arXiv:1909.07507*, 2019.
- [21] M. Lisotto, P. Coscia, and L. Ballan, “Social and scene-aware trajectory prediction in crowded spaces,” in *Proceedings of the IEEE International Conference on Computer Vision Workshops*, 2019, pp. 0–0.
- [22] N. Lee, W. Choi, P. Vernaza, C. B. Choy, P. H. Torr, and M. Chandraker, “Desire: Distant future prediction in dynamic scenes with interacting agents,” in *Proceedings of the IEEE Conference on Computer Vision and Pattern Recognition*, 2017, pp. 336–345.
- [23] Y. Zhu, D. Qian, D. Ren, and H. Xia, “Starnet: Pedestrian trajectory prediction using deep neural network in star topology,” *arXiv preprint arXiv:1906.01797*, 2019.
- [24] J. Amirian, J.-B. Hayet, and J. Pettré, “Social ways: Learning multi-modal distributions of pedestrian trajectories with gans,” in *Proceedings of the IEEE Conference on Computer Vision and Pattern Recognition Workshops*, 2019, pp. 0–0.
- [25] X. Chen, Y. Duan, R. Houthoofd, J. Schulman, I. Sutskever, and P. Abbeel, “Infogan: Interpretable representation learning by information maximizing generative adversarial nets,” in *Advances in neural information processing systems*, 2016, pp. 2172–2180.
- [26] W.-C. Ma, D.-A. Huang, N. Lee, and K. M. Kitani, “Forecasting interactive dynamics of pedestrians with fictitious play,” in *Proceedings of the IEEE Conference on Computer Vision and Pattern Recognition*, 2017, pp. 774–782.
- [27] Y. Li, “Which way are you going? imitative decision learning for path forecasting in dynamic scenes,” in *Proceedings of the IEEE Conference on Computer Vision and Pattern Recognition*, 2019, pp. 294–303.

- [28] T. van der Heiden, N. S. Nagaraja, C. Weiss, and E. Gavves, “Safecritic: Collision-aware trajectory prediction,” *arXiv preprint arXiv:1910.06673*, 2019.
- [29] N. Deo and M. M. Trivedi, “Scene induced multi-modal trajectory forecasting via planning,” *arXiv preprint arXiv:1905.09949*, 2019.
- [30] T. Fernando, S. Denman, S. Sridharan, and C. Fookes, “Neighbourhood context embeddings in deep inverse reinforcement learning for predicting pedestrian motion over long time horizons,” in *Proceedings of the IEEE International Conference on Computer Vision Workshops*, 2019, pp. 0–0.
- [31] D. Helbing and P. Molnar, “Social force model for pedestrian dynamics,” *Physical review E*, vol. 51, no. 5, p. 4282, 1995.
- [32] S. Yi, H. Li, and X. Wang, “Understanding pedestrian behaviors from stationary crowd groups,” in *Proceedings of the IEEE Conference on Computer Vision and Pattern Recognition*, 2015, pp. 3488–3496.
- [33] A. Sadeghian, V. Kosaraju, A. Sadeghian, N. Hirose, H. Rezaatofghi, and S. Savarese, “Sophie: An attentive gan for predicting paths compliant to social and physical constraints,” in *Proceedings of the IEEE Conference on Computer Vision and Pattern Recognition*, 2019, pp. 1349–1358.
- [34] V. Kosaraju, A. Sadeghian, R. Martín-Martín, I. Reid, H. Rezaatofghi, and S. Savarese, “Social-bigat: Multimodal trajectory forecasting using bicycle-gan and graph attention networks,” in *Advances in Neural Information Processing Systems*, 2019, pp. 137–146.
- [35] Y. Huang, H. Bi, Z. Li, T. Mao, and Z. Wang, “Stgat: Modeling spatial-temporal interactions for human trajectory prediction,” in *Proceedings of the IEEE International Conference on Computer Vision*, 2019, pp. 6272–6281.
- [36] Y. Ma, X. Zhu, S. Zhang, R. Yang, W. Wang, and D. Manocha, “Trafficpredict: Trajectory prediction for heterogeneous traffic-agents,” in *Proceedings of the AAAI Conference on Artificial Intelligence*, vol. 33, 2019, pp. 6120–6127.
- [37] B. Ivanovic and M. Pavone, “The trajectron: Probabilistic multi-agent trajectory modeling with dynamic spatiotemporal graphs,” in *Proceedings of the IEEE International Conference on Computer Vision*, 2019, pp. 2375–2384.
- [38] L. Zhang, Q. She, and P. Guo, “Stochastic trajectory prediction with social graph network,” *arXiv preprint arXiv:1907.10233*, 2019.
- [39] C. Tang and R. R. Salakhutdinov, “Multiple futures prediction,” in *Advances in Neural Information Processing Systems*, 2019, pp. 15 398–15 408.
- [40] E. Denton and R. Fergus, “Stochastic video generation with a learned prior,” in *International Conference on Machine Learning*, 2018, pp. 1182–1191.
- [41] D. P. Kingma and J. Ba, “Adam: A method for stochastic optimization,” *arXiv preprint arXiv:1412.6980*, 2014.